# Retinopathy in a novel model of metabolic syndrome and type 2 diabetes: new insight on the inflammatory paradigm

**Kousuke Noda,[*,‡,1] Shintaro Nakao,[*,†,§,1] Souska Zandi,[*,†,1] Dawei Sun,[*,†,‖] K. C. Hayes,[¶] and Ali Hafezi-Moghadam[*,†,2]**

[*]Center for Excellence in Functional and Molecular Imaging, Brigham and Women's Hospital, Boston, Massachusetts, USA; [†]Department of Radiology, Harvard Medical School, Boston, Massachusetts, USA; [‡]Department of Ophthalmology, Hokkaido University Graduate School of Medicine, Sapporo, Japan; [§]Department of Ophthalmology, Graduate School of Medical Sciences, Kyushu University, Fukuoka, Japan; [‖]Department of Ophthalmology, Second Affiliated Hospital of Harbin Medical University, Harbin, China; and [¶]Foster Biomedical Research Laboratory, Department of Biology, Brandeis University, Waltham, Massachusetts, USA

ABSTRACT **The pathogenesis of diabetic retinopathy (DR) in metabolic syndrome (MetS) and type 2 diabetes (T2D) is not well studied, partly because an appropriate model has not been developed. Recently, we introduced a novel model of spontaneous T2D and MetS that replicates the relevant features of the human disease. In the current study, we investigated the retinal vascular changes in these animals. Experimental DR in streptozotocin (STZ)-injected rodents is described as an inflammatory disease, in which intercellular adhesion molecule 1 (ICAM-1) plays a key role. In comparison, advanced diabetes (HbA1c>10%) in the Nile grass rat (NGR) was associated with lower ICAM-1 protein expression when compared with that in normal or moderately diabetic animals. Vascular cell adhesion molecule 1 (VCAM-1) expression, however, was unaffected by the disease state. As opposed to the STZ-induced model of DR, in diabetic NGRs, most leukocytes accumulated in the retinal arteries. Consistent with the ICAM-1 reduction, leukocyte accumulation was significantly reduced in advanced disease. Similarly, leukocyte adhesions were significantly lower, with elevated plasma triglycerides (>200 mg/dl), and cholesterol (>240 mg/dl). However, these adhesions were significantly higher in animals with higher plasma insulin (>5 μIU/ml) and leptin (>20 ng/ml), suggesting a role for these hormones in diabetic retinal leukostasis. Diabetic NGRs showed substantial retinal endothelial injury, primarily in the microvessels, including vascular tortuosity, obliterated acellular capillaries, and pericyte ghosts. The NGR provides a convenient and realistic model for investigation of retinal changes in MetS/T2D with convincing advantages over the commonly used STZ-induced T1D.— Noda, K., Nakao, S., Zandi, S., Sun, D., Hayes, K. C., Hafezi-Moghadam, A. Retinopathy in a novel model of metabolic syndrome and type 2 diabetes: new insight on the inflammatory paradigm. *FASEB J.* 28, 2038–2046 (2014). www.fasebj.org**

*Key Words: adhesion molecules · adipokines · Nile grass rat*

Currently, there is a growing epidemic of metabolic syndrome (MetS) and type 2 diabetes (T2D) in industrialized and developing countries. MetS is characterized by the variable coexistence of abdominal obesity, dyslipidemia, hyperinsulinemia, and hypertension (1, 2). When insulin-resistant individuals fail to maintain the hyperinsulinemia needed to keep a normal blood glucose (BG) level, fulminant disease ensues (3). MetS is associated with a markedly increased risk of the development of diabetic complications. A debilitating complication and a leading cause of vision loss is diabetic retinopathy (DR; ref. 4). Currently, there is no satisfactory model for the study of the pathogenesis of DR in MetS/T2D.

Streptozotocin (STZ)-induced hyperglycemia is commonly used in retinal research; however, the great need to reach beyond hyperglycemia has been recognized (5). Existing T2D models include the ob/ob mouse (6), the KK mouse (7), the db/db mouse (8), the Goto-Kakizaki (GK) rat (9), the Wistar fatty rat (10), the Otsuka-Long-Evans-Tokushima fatty (OLETF) rat (11), the Torii nonobese rat (12), and the morbidly obese desert sand rat (13). These models have contributed

Abbreviations: BG, blood glucose; BRB, blood–retina barrier; BW, body weight; ConA, concanavalin A; DR, diabetic retinopathy; EB, Evans blue; FITC, fluorescein isothiocyanate; HbA1c, hemoglobin A1c; ICAM-1, intercellular adhesion molecule 1; MetS, metabolic syndrome; NGR, Nile grass rat; PBS, phosphate-buffered saline; PI, propidium iodide, STZ, streptozotocin; T1D, type 1 diabetes; T2D, type 2 diabetes; TG, triglyceride; VCAM-1, vascular cell adhesion molecule 1

[1] These authors contributed equally to this work.

[2] Correspondence: Brigham & Women's Hospital, 221 Longwood Avenue, Boston, MA 02115, USA. E-mail: ahm@bwh.harvard.edu

doi: 10.1096/fj.12-215715



0892-6638/14/0028-2038 © FASEB

significantly to our understanding of diabetes and its organ manifestations, whereas no single model sufficiently encompasses the entire complexity of the human disease.

Early DR is characterized by microvascular damage secondary to capillary nonperfusion (14). The vascular damage has been linked to inflammation; however, details of the pathogenesis remain to be studied. In early DR, inflammatory cells accumulate in retinal vessels (15). Endothelial intercellular adhesion molecule 1 (ICAM-1) interaction with leukocyte β2-integrins is critical to firm adhesion. The retinal endothelium in animals with STZ-induced diabetes expresses more ICAM-1 (16–18), which is thought to facilitate the trapping of leukocytes in capillaries and lead to nonperfusion. The role of ICAM-1 in DR, however, remains controversial, as both elevated (18) and unaltered (19) ICAM-1 levels have been reported in tissues of diabetic patients. Furthermore, a significant portion of ICAM-1 is found in the choroidal vessels (18).

The increased ICAM-1 found in animals with STZ-induced diabetes does not sufficiently address the role of this molecule in DR, because STZ-induced animals model the hyperglycemia of type 1 diabetes (T1D), whereas human T2D is more complex, involving an array of metabolic and hormonal changes (20). Although plasma glucose is elevated in both T1D and T2D, the role of insulin, adiponectin, and lipids in DR development remain to be elucidated. Chen *et al.* (21) reported that dyslipidemia, not hyperglycemia, induces inflammatory adhesion molecules in human retinal vascular endothelial cells. To understand the impact of lipids, insulin, and adipokines on retinal disease, better models of DR are needed.

A concern of the commonly used STZ-induced model of DR is the direct toxic effect of the drug on endothelial cells (22). Another concern is that, in STZ-induced diabetes, most leukocytes adhere within the postcapillary venules, rather than within the arteries (23, 24). These leukocytes, by virtue of their adhesion beyond the capillaries, would not explain the phenomenon of capillary plugging and nonperfusion and the fact that arterial changes are associated with the risk of DR development in humans (25). Therefore, it is unclear to what extent the insights gained from the STZ-treated animals with respect to ICAM-1 and leukocyte accumulation in the retinal veins can be applied to the human disease.

In following the physiological, nutritional, and pathologic parameters of more than 2500 Nile grass rats (NGRs) over the past 6+ years, we have discovered that the NGR is metabolically challenged in much the same way as humans with T2D and MetS, developing disease even when fed standard lab chow (20, 26, 27). The data collected from these animals allowed us to establish a novel carbohydrate-induced model of metabolic syndrome in NGRs that mimics the dietary situation in humans (27). The NGR, *Arvicanthis niloticus,* is an herbivorous rodent inhabiting the dry savanna, woodlands, and grasslands in Africa (20, 26). They live underground in burrows constructed of a central area with surface runways radiating outward. As opposed to other rodent species that are nocturnal, NGRs are primarily diurnal. This unique behavioral pattern has made NGRs a valuable tool in the study of circadian rhythm. Furthermore, they express ~35% cones in their retina and thus offer a unique opportunity for the study of photoreceptors. Most important, our new model shows all the relevant hallmarks of human metabolic syndrome: insulin resistance, dyslipidemia, and hypertension (20).

In a prior study, we established the relation between plasma adiponectin and insulin in NGRs, in the various stages of the diabetic progression, including the prediabetic, hyperinsulinemic, and full-blown, late-stage disease (20). To our knowledge, no other spontaneous diabetes in rodents offers a more suitable model of human MetS/T2D for the study of retinal changes in relation to these important parameters. In this report, the impact of MetS/T2D on retinal vessels is described in terms of the dynamic changes in local and systemic parameters.

## MATERIALS AND METHODS

### Animals

All animal experiments were approved by the institutional Animal Care Committees of Brandeis University and the Massachusetts Eye and Ear Infirmary and adhered to Association for Research in Vision and Ophthalmology (ARVO) and Association for Assessment and Accreditation of Laboratory Animal Care International (AAALAC) regulations for the care and use of animals. NGRs were bred in the Brandeis University facility and housed in ventilated plastic cages in a temperature-controlled environment with a 12-h light/dark cycle. The animals were fed standard laboratory chow (Lab Diet 5020; PMI Nutrition, St. Louis, MO, USA) and water *ad libitum.* The animals in this study were from wild-type breeders, and most male pups are prone to MetS and T2D within 4–6 wk after weaning (20, 26, 27).

### Western blot analysis

To obtain tissues, we perfused the animals with phosphate-buffered saline (PBS) and enucleated the eyes immediately after perfusion. The retinas were microsurgically isolated and placed in 100 μl of lysis buffer (mammalian cell lysis kit MCL1; Sigma-Aldrich, St. Louis, MO, USA), supplemented with protease and phosphatase inhibitors (P2850, P5726, and P8340; Sigma-Aldrich), and sonicated. The lysate was centrifuged (12,000 rpm, 15 min, and 4°C), and the supernatant was collected. Each sample containing an equal amount of total protein, quantified by protein assay (Bio-Rad Laboratories, Hercules, CA, USA), was separated by SDS-PAGE and electroblotted onto polyvinylidene fluoride (PVDF) membranes (Invitrogen-Life Technologies, Carlsbad, CA, USA). To block nonspecific binding, the membranes were washed with 5% skim milk and subsequently incubated with Abs against ICAM-1Ab (5 μg/ml, M-19; sc-1511; Santa Cruz Biotechnology, Santa Cruz, CA, USA), vascular cell adhesion molecule 1 Ab (VCAM-1Ab; 5 μg/ml, H-276; sc-8304; Santa Cruz Biotechnology), and β-tubulin (ab11308; Abcam, Cambridge, MA, USA) at 4°C overnight, followed by incubation with a horseradish peroxidase–conjugated donkey or sheep Ab against rabbit or mouse IgG (NA934V and NXA931; GE Healthcare, Piscataway, NJ, USA). The signals

were visualized by chemiluminescence (ECL kit; GE Healthcare), according to the manufacturer's protocol.

### Concanavalin A (ConA) lectin staining of adherent leukocytes

The chest cavity was opened in rats under deep anesthesia, and the left ventricle was cannulated to allow perfusion (20). The right atrium was opened to achieve outflow. PBS (20 ml) was perfused to clear erythrocytes and nonsticking leukocytes, followed by 20 ml of fluorescein isothiocyanate (FITC)-coupled ConA lectin (20 μg/ml in PBS, pH 7.4; total concentration 5 mg/kg; Vector Laboratories, Burlingame, CA, USA), which stains adherent leukocytes and the vascular endothelium. The animals were then perfused with PBS alone for 4 min to remove excess ConA. The eyes were enucleated, and the retinas were dissected and flat mounted in a water-based, fluorescent, antifade medium (Fluoromount; Southern Biotechnology, Birmingham, AL, USA) and imaged by fluorescence microscopy (FITC filter; Leica Microsystems, Buffalo Grove, IL, USA). Only whole retinas in which the peripheral collecting vessels of the ora serrata were visible were used in the analysis. Leukocytes in the arteries, veins, and capillaries of each retinal tissue were counted in a radius of 3 mm around the optic nerve, and the total number of adherent leukocytes per retina was calculated.

### Immunohistochemistry

Eyes were enucleated and fixed with 4% paraformaldehyde for 30 min at 4°C. For whole-mount preparation, the retinas were microsurgically exposed by removing other portions of the eye. The retinas were washed with PBS 3 times for 5 min each and then placed in methanol for 20 min. The tissues were incubated overnight at 4°C with anti-ICAM-1 Ab (5 μg/ml, M-19; sc-1511; Santa Cruz Biotechnology) and anti-VCAM-1Ab (5 μg/ml, H-276; sc-8304; Santa Cruz Biotechnology), diluted in PBS containing 10% goat serum and 1% Triton X-100. The tissues were then washed 4 times in PBS for 20 min, followed by incubation with ICAM-1: Alexa Fluor488 donkey anti-goat IgG (20 μg/ml, A11055; Invitrogen); VCAM-1: Alexa Fluor488 goat anti-rabbit IgG (20 μg/ml, A11008; Invitrogen) overnight at 4°C. Retinal flat mounts were prepared on glass slides in a mounting medium (TA-030-FM; Permafluor; Lab Vision Corp., Fremont, CA, USA).

### Quantification of firm leukocyte adhesion in retinal vessels

The retinal vasculature and adherent leukocytes were imaged with FITC-coupled ConA lectin (Vector Laboratories). Animals were deeply anesthetized, and the chest cavity was carefully opened. A 14-gauge perfusion cannula was introduced into the aorta. After drainage was achieved from the right atrium, the animals were perfused with PBS at 500 ml/kg body weight (BW), to remove erythrocytes and nonadherent leukocytes. Perfusion with ConA (40 μg/ml in PBS, pH 7.4, and 5 mg/kg BW) was performed to label adherent leukocytes and vascular endothelial cells, followed by removal of residual unbound lectin with PBS perfusion. The retinas were carefully removed and flat mounted in a mounting medium for fluorescence (Vector Laboratories). Each retina was imaged with an epifluorescence microscope (DM RXA; Leica Microsystems), and the total number of adherent leukocytes per retina was determined.

### Hemoglobin A1c (HbA1c), BG, triglyceride (TG), adiponectin, insulin, and plasma lipid measurements

BG levels in rats were measured from tail blood samples, taken randomly or after 16 h overnight food deprivation, with an Elite Glucometer (Bayer, Elkhart, IN, USA). Animals with repeated BG 150 mg/dl were considered diabetic. After 3–5 d, the animals were deeply anesthetized, and blood was collected by cardiac puncture, into EDTA-treated syringes. Glycated hemoglobin (GHb) was measured by a Glyco-Tek affinity column kit (Helena Laboratories, Beaumont, TX, USA). HbA1c was calculated according to the equation provided by the manufacturer. Animals with HbA1c 6.5% were considered diabetic, in accordance with the diabetes management guidelines of the American College of Endocrinology (22, 23). Subsequently, blood was centrifuged at 12,000 *g* for 10 min at 4°C, and plasma was collected. Plasma levels of total cholesterol (TC) and TGs were measured by the enzymatic assay provided in the Thermo Infinity kit (ThermoElectron, Pittsburgh, PA, USA).

#### *Quantification of blood–retina (BRB) barrier permeability in NGRs*

Retinal vascular permeability was quantified as described previously (28). Briefly, under deep anesthesia, Evans blue (EB) dye (30 mg/ml in saline; E2129; Sigma-Aldrich) was injected through the femoral vein at 45 mg/kg. After the dye had circulated for 2 h, blood samples were obtained from the left ventricle to obtain the time-averaged EB plasma concentration. Blood samples were centrifuged at 12,000 rpm for 15 min to separate the plasma from the cellular components. Plasma samples were then diluted to 1:10,000 of their initial concentration in formamide (Sigma-Aldrich). Absorbance was measured with a spectrophotometer at 620 and 740 nm. Subsequently, the chest cavity was opened, and the rats were perfused through the left ventricle with paraformaldehyde 1% (158127; Sigma-Aldrich) in citrate buffer (0.05 M, pH 3.5; P4809; Sigma-Aldrich). The retinas were then dissected under an operating microscope, and their weight was determined. To extract the EB, the retinas were incubated in 180 μl formamide for 24 h (F9037; Sigma-Aldrich). The extract was ultracentrifuged at a speed of 14,000 rpm for 60 min. The supernatant (60 μl) was used for spectrophotometric measurements. Background-subtracted absorbance was determined by measuring each sample at 620 nm (absorbance maximum for EB in formamide) and 740 nm (absorbance minimum). BRB breakdown was calculated and the values expressed as plasma (μl) × retinal weight ($g^{-1}$) × time ($h^{-1}$).

#### *Trypsin digestion and analysis of retinal vasculature*

Eyes from normal and diabetic NGRs ($n$=4/group) were enucleated and fixed in 10% neutral buffered formalin. The eyes were placed in 6-well plates in PBS. The retinas were then dissected under a surgical microscope and washed 4–5 times with filtered water, to facilitate the separation of the neural retinal layers from the blood vessels. Subsequently, the retinas were incubated in 0.1 M Tris buffer (T8193, pH 7.8; Sigma-Aldrich) containing 3% trypsin (Difco 1:250; 0458; Amresco LLC, Solon, OH, USA) at 37°C for 90 min. Water washes were used to disintegrate the neuronal tissues and debris from the vascular network. The retinal vascular network was then flat mounted on a slide and stained with periodic acid solution (PAS, 3951; Sigma-Aldrich), Schiff's reagent (3952016; Sigma-Aldrich), and hematoxylin (GHS316; Sigma-Aldrich).

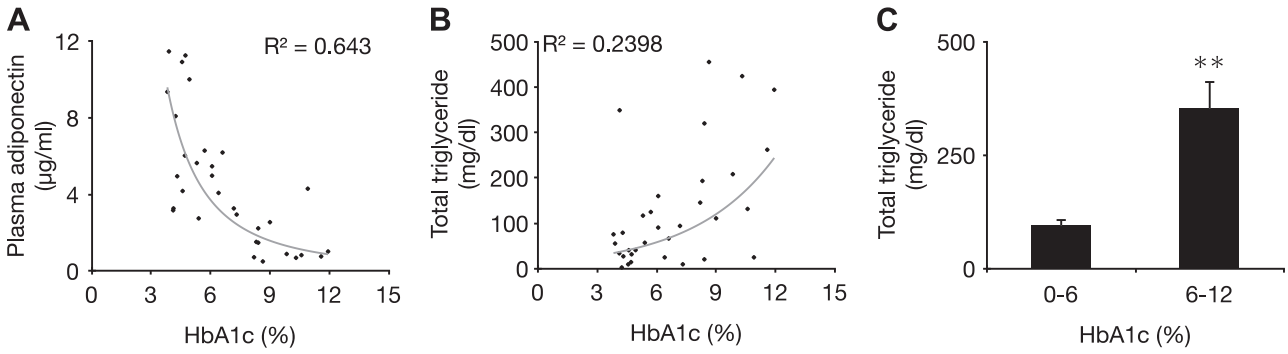


**Figure 1.** Metabolic characteristics of the NGR. *A*) Adiponectin is a key indicator of the metabolic state. Negative correlation between plasma adiponectin and plasma HbA1c in NGRs shows the close resemblance of this model with the human T2D and MetS. *B*) Distribution of plasma TG levels in relation to plasma HbA1c as an indicator of disease state in NGRs. *C*) Total plasma TGs in normal (<6%) and diabetic (>6% HbA1C) NGRs. $^{**}P < 0.01$.

### Statistical analysis

All values are expressed as means ± SEM. Student's *t* test was used for statistical analysis. Differences between the experimental groups were considered statistically significant at $P < 0.05$.

## RESULTS

### Metabolic levels in the examined animals

As an important hormonal correlate of the metabolic state, non-food-deprived levels of plasma adiponectin were measured in the animals that were subsequently used for retinal analysis. Plasma adiponectin correlated inversely with HbA1c (**Fig. 1*A***). By contrast, plasma TGs correlated positively with HbA1c (Fig. 1*B*), in line with our original observation in a larger population (20, 26). Plasma TGs in the normal nondiabetic controls (HbA1c<6%) were within normal range and significantly lower than in the diabetic (HbA1c<6%) animals, confirming the fidelity of this aspect of the model to the human MetS/T2D (Fig. 1*C*).

### Lower ICAM-1 expression in advanced disease

ICAM-1 is up-regulated in STZ-induced diabetes and thus is thought to be mechanistically involved in DR pathogenesis (17). Staining for ICAM-1 in normal and diabetic NGRs revealed that the molecule was present in the retinal vessels of the animals (**Fig. 2*A***). Since little is known about the dynamics of ICAM-1 expression in MetS/T2D, ICAM-1 in retinas of the NGRs was measured and found comparable in the normal (HbA1c <6%) and diabetic (HbA1c 6–10%) animals. In the animals with late-stage disease (HbA1c >10%), ICAM-1 was substantially reduced (Fig. 2*B*). Indeed beyond an HbA1c of 6%, ICAM-1 correlated negatively with HbA1c (Fig. 2*C*). When ranked in subgroups by HbA1c, there was no difference between the normal (HbA1c <6%) and the diabetic (HbA1c 6–10%) animals, whereas the advanced diabetic rats (HbA1c >10%) showed significantly lower ICAM-1 levels (Fig. 2*D*).

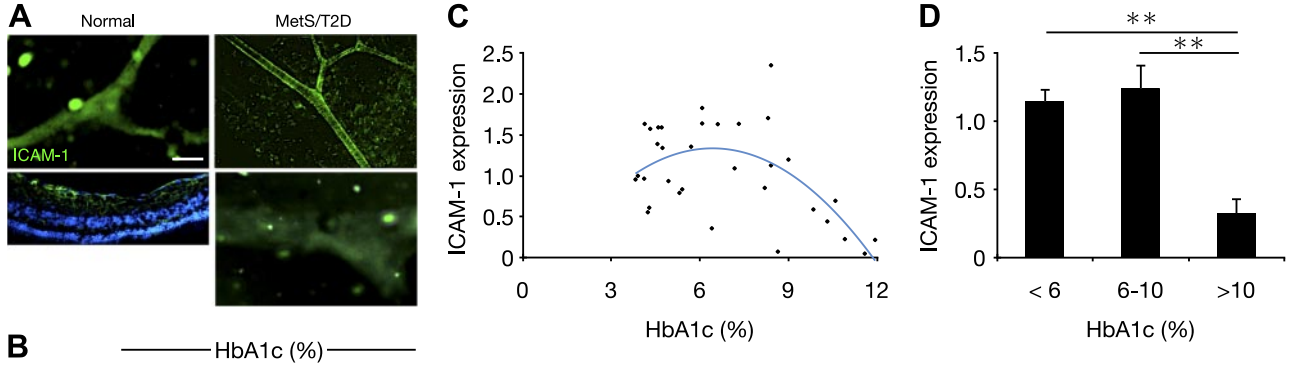


**Figure 2.** Dynamic of ICAM-1 expression in retinas of NGR. *A*) Immunohistochemistry for ICAM-1 in retinal vessels of normal (<6% HbA1c, left) and diabetic NGR (6–10% HbA1c, top right), and late stage disease (>10% HbA1c, bottom right micrograph) Scale bar = 50 μm. *B*) Representative Western blot bands for ICAM-1 and β-tubulin in normal (<6%), diabetic (6–10%), and late-stage (>10% HbA1c) diabetic animals. *C*) Distribution of retinal ICAM-1 expression in relation to plasma HbA1c. *D*) Quantitative analysis of Western blots of retinal ICAM-1 in normal (<6%), diabetic (6–10%), and late-stage (>10% HbA1c) diabetic animals. Standardization was determined as the ratio of the ICAM-1 band densities through the respective β-tubulin internal control bands. $^{**}P < 0.01$.

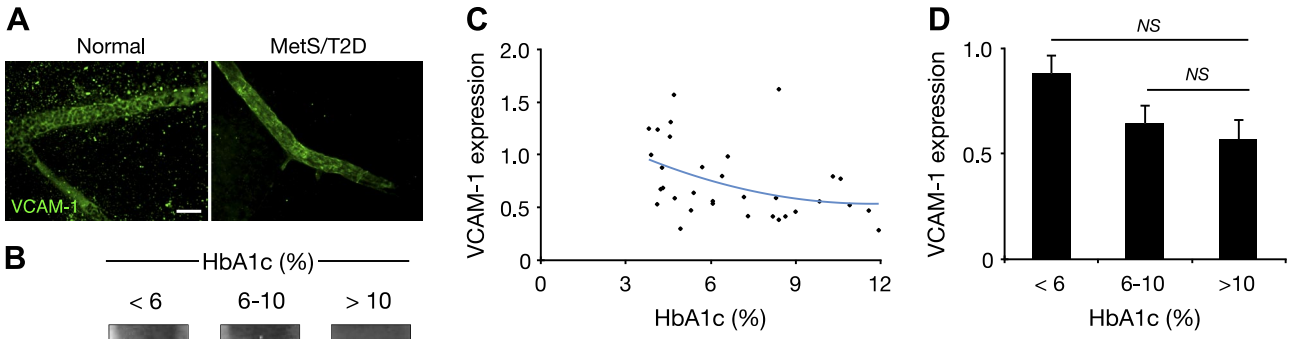


**Figure 3.** Unchanged VCAM-1 in retinas of NGRs. *A*) Immunohistochemistry for VCAM-1 in retinal vessels of normal (<6% HbA1c) and diabetic NGRs (6–10% HbA1c). Scale bar = 30 μm. *B*) Representative Western blot bands for VCAM-1 and β-tubulin in normal (<6%), diabetic (6–10%), and late-stage diabetic (>10% HbA1c) animals. *C*) Distribution of retinal VCAM-1 expression in relation to plasma HbA1c. *D*) Quantitative analysis of retinal VCAM-1 in normal (<6%), diabetic (6–10%), and late-stage diabetic (>10% HbA1c) animals. NS, not significant.

### Unchanged VCAM-1 with disease progression

As a comparison with another important endothelial injury marker, we examined VCAM-1 expression in the retinas of the same NGRs. Retinal vessels of the normal and MetS/T2D animals showed positive staining for VCAM-1 (**Fig. 3*A***). When measured in Western blots, VCAM-1 was at comparable levels in the normal (HbA1c <6%), diabetic (HbA1c 6–10%), and late-stage (HbA1c >10%) animals (Fig. 3*B*). However, as opposed to ICAM-1, no correlation was observed between VCAM-1 and HbA1c levels (Fig. 3*C*). That rats with advanced diabetes (HbA1c >10%) showed no significant difference in VCAM-1 expression with normal and diabetic animals suggests that reduced endothelial density *per se* is not the cause of lower adhesion molecule expression (Fig. 3*D*).

### Surprising inverse relation of leukocyte accumulation with disease progression

DR is an inflammatory disease, and leukocyte accumulation is considered an early mechanistic event (17). When firm leukocyte adhesion was measured in the normal and diabetic/metabolic NGRs, few leukocytes were found to adhere firmly to the retinal vessels. In the diabetic animals, firmly adhering leukocytes were found, but surprisingly, they occurred mostly in the retinal arteries, not in the veins (**Fig. 4*A***). Furthermore, there was a negative correlation between leukocyte accumulation in arteries and the state of disease (Fig. 4*B*). Indeed, the number of firmly adhering leukocytes in animals with advanced disease (HbA1c >10%) was significantly lower than in the normal control (HbA1c <6%) or diabetic (HbA1c 6–10%) animals (Fig. 4*C*).

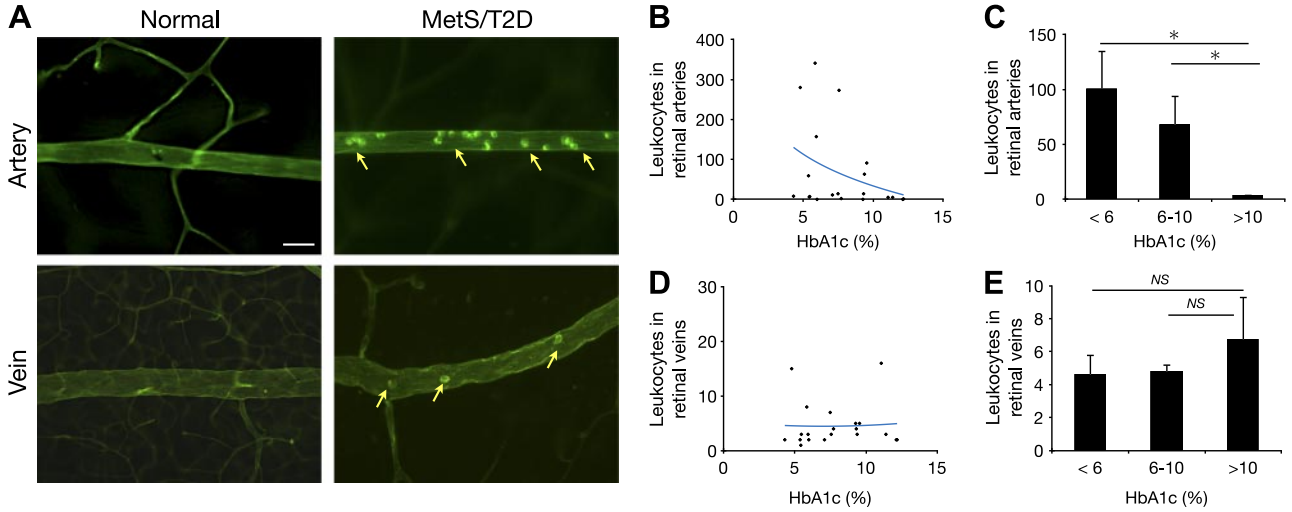


**Figure 4.** Retinal arterial leukostasis in diabetic animals. Characterization of retinal inflammation in normal and diabetic animals. *A*) Visualization of leukostasis in retinal vessels during diabetes. Micrographs show representative ConA staining in retinas of normal and diabetic animals. Arrows depict firmly adhering leukocytes. Scale bar = 30 μm. *B*) Distribution of leukocytes in retinal arteries in relation to HbA1c. *C*) Quantitative analysis of arterial leukocytes in normal (<6%), diabetic (6–10%), and late-stage diabetic (>10% HbA1c) animals. *D*) Distribution of the leukocytes in retinal veins in relation to HbA1c. *E*) Quantitative analysis of the venous leukocyte accumulation in normal (<6%), diabetic (6–10%), and late-stage diabetic (>10% HbA1c) animals. $^*P < 0.05$.

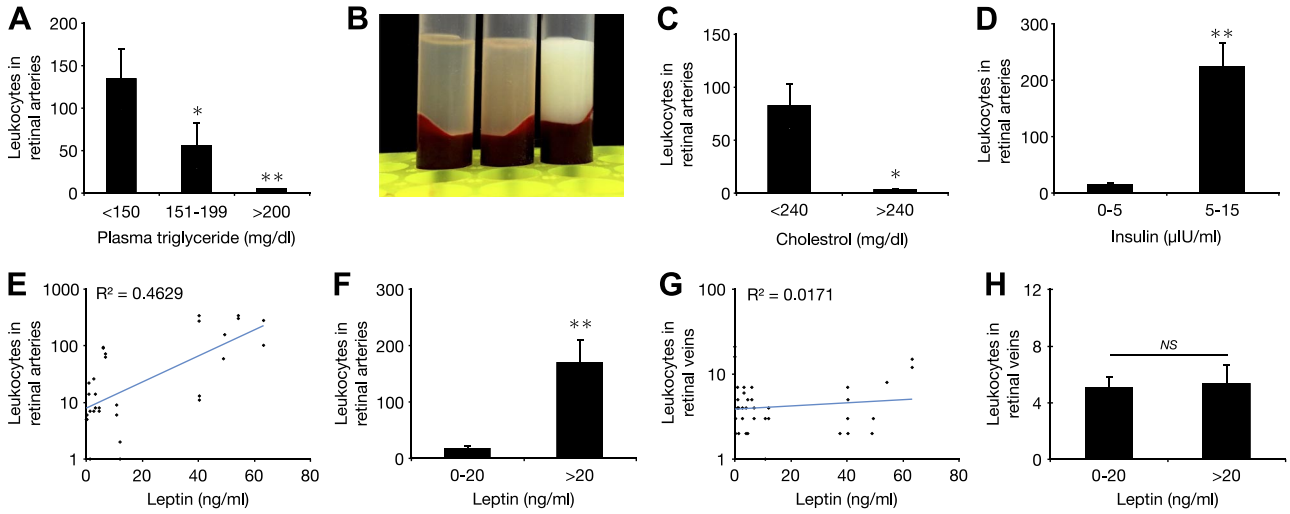


**Figure 5.** Relation of metabolic parameters and cellular inflammation. *A*) Retinal arterial leukocyte accumulation in relation to plasma TGs. Compared to normal (<150 mg/dl), arterial leukocyte accumulation was significantly lower in animals with marginally increased plasma TG (151–199 mg/dl) and further reduced in animals with markedly increase plasma TG (>200 mg/dl). *B*) Representative plasmas, from left to right: normal (transparent) and moderately and strongly hypertriglyceridemic animals (white opaque). *C*) Retinal leukocyte accumulation in animals with normal (<240 mg/dl) *vs.* animals with elevated plasma cholesterol levels (>240 mg/dl). *D*) Number of retinal arterial leukocytes in relation to fasting plasma insulin level. *E*) Distribution of leukocytes in retinal arteries in relation to plasma leptin. *F*) Number of retinal arterial leukocytes in relation to plasma leptin. *G*) Distribution of the leukocytes in retinal veins in relation to plasma leptin. *H*) Number of retinal venous leukocytes in relation to plasma leptin. $^*P < 0.05$; $^{**}P < 0.01$.

In comparison, in the retinal veins, there was no correlation between leukocyte accumulation and HbA1c (Fig. 4*D*) (*i.e.*, between the normal, diabetic, or advanced diabetic animals; Fig. 4*E*).

### Characterization of metabolic parameters in retinal inflammation

The role of lipids and adipokines, in DR is not well understood. We measured plasma TGs and quantified leukocyte accumulation. The number of firmly adhering leukocytes was significantly lower in the animals with slightly (151–199 mg/dl) or greatly elevated plasma TGs (>200 mg/dl) compared with that in the normal animals (**Fig. 5*A***). Examples of low, medium, and high plasma TG levels are illustrated by the opacity and color of the plasma from freshly obtained blood samples (Fig. 5*B*). Similarly, hypercholesterolemia (>240 mg/dl) resulted in significantly less leukocyte adhesion compared to that in the nondiabetic rats with normal cholesterol levels (Fig. 5*C*). Leukocyte adhesion was significantly increased by hyperinsulinemia (>5 μIU/ml), compared to that in the normoinsulinemic animals (<5 μIU/ml) (Fig. 5*D*). Leptin values correlated positively with retinal arterial leukocyte adhesions (Fig. 5*E*). Leukocyte adhesions were significantly higher in the animals with higher leptin values compared to that in the normal animals (Fig. 5*F*). In contrast, plasma leptin did not correlate with retinal venous leukocyte adhesions (Fig. 5*G*, *H*).

### Increased BRB permeability in MetS/T2D NGRs

To evaluate the BRB function in the diabetic animals, we used the EB technique (28). In the MetS/T2D animals, we observed significantly higher leakage into the retinal tissue, compared to that in the normal animals (**Fig. 6**). In T1D, the BRB breakdown in diabetes is thought to be a mechanistic consequence of leukocyte adhesion (28). The current results, however, indicate that other factors, aside from leukocyte accumulation in MetS/T2D, may contribute to the BRB breakdown.

### Increased endothelial damage with disease progression

Next, we investigated cellular injury in retinas of the NGRs. In the normal animals, no endothelial propidium iodide (PI) staining was observed (**Fig. 7*A***). In contrast, the diabetic animals showed significantly more PI-positive cells that could be endothelial cells or pericytes (Fig. 7*B*, *C*). Notably, most of the PI-positive cells were observed in the microvessels, when compared with the number in the larger vessels (Fig. 7*D*).

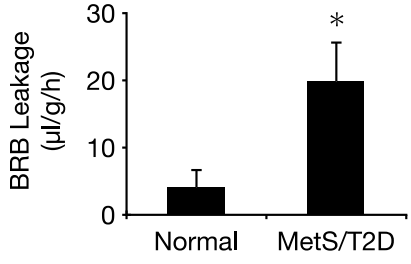


**Figure 6.** Retinal vascular leakage in normal and diabetic animals. BRB was evaluated in normal (<6% HbA1c) and diabetic (6–10% HbA1c) animals with the EB technique ($n$=3/group). $^*P < 0.05$.

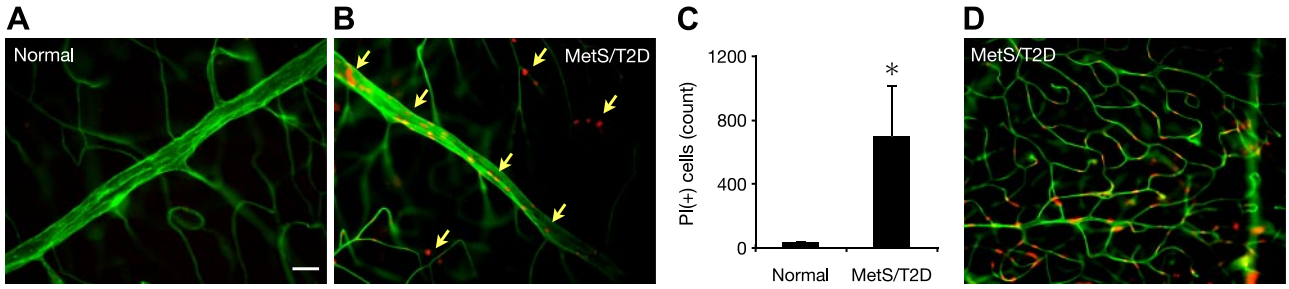


**Figure 7.** Cellular injury in diabetic NGRs. Retinal endothelial cell damage was detected with PI (red) staining in normal and diabetic NGRs. Vasculature was stained with FITC-ConA (green). *A*) Normal NGR lacking PI-positive staining, indicative of healthy vasculature (6-mo-old male, BW 104.6 g, BG 74 mg/dl, HbA1c 4.8%). Scale bar = 30 μm. *B*) A representative diabetic NGR (6-mo-old female, BW 90.5 g, BG 473 mg/dl, HbA1c 8.4%) showing PI-positive staining, indicative of cell death. *C*) Quantification of PI-positive cells in the retinas of normal and diabetic NGRs ($n$=4/group) *$P < 0.05$. *D*) PI-positive endothelial cells or pericytes in the retinal microvessels of a diabetic NGR, indicating early cellular damage.

### Structural abnormalities in MetS/T2D NGRs

To further investigate microvascular changes, we performed trypsin digestion of the retinas of the normal and diabetic animals. Retinas of the nondiabetic NGRs showed patent capillaries with endothelial cells and the surrounding pericytes (**Fig. 8*A*** and ref. 29). In contrast, MetS/T2D NGR showed numerous obliterated, acellular capillaries, a classic sign of DR (Fig. 8*B*). In addition, MetS/T2D NGR retinas showed vascular anomalies that fit the description of pericyte ghosts (Fig. 8*C* and ref. 30) and other irregularities of the microvascular wall (Fig. 8*D*). In retinal flat mounts of the FITC-ConA–perfused NGRs, we found widened arterial regions in the diabetic NGRs that were not found in the normal ones (Fig. 8*E*) or in the STZ-induced diabetic animals (data not shown). Incidentally, these vascular regions coincided with increased leukocyte accumulations (Fig. 8*E*). As a structural abnormality, irregular venous walls

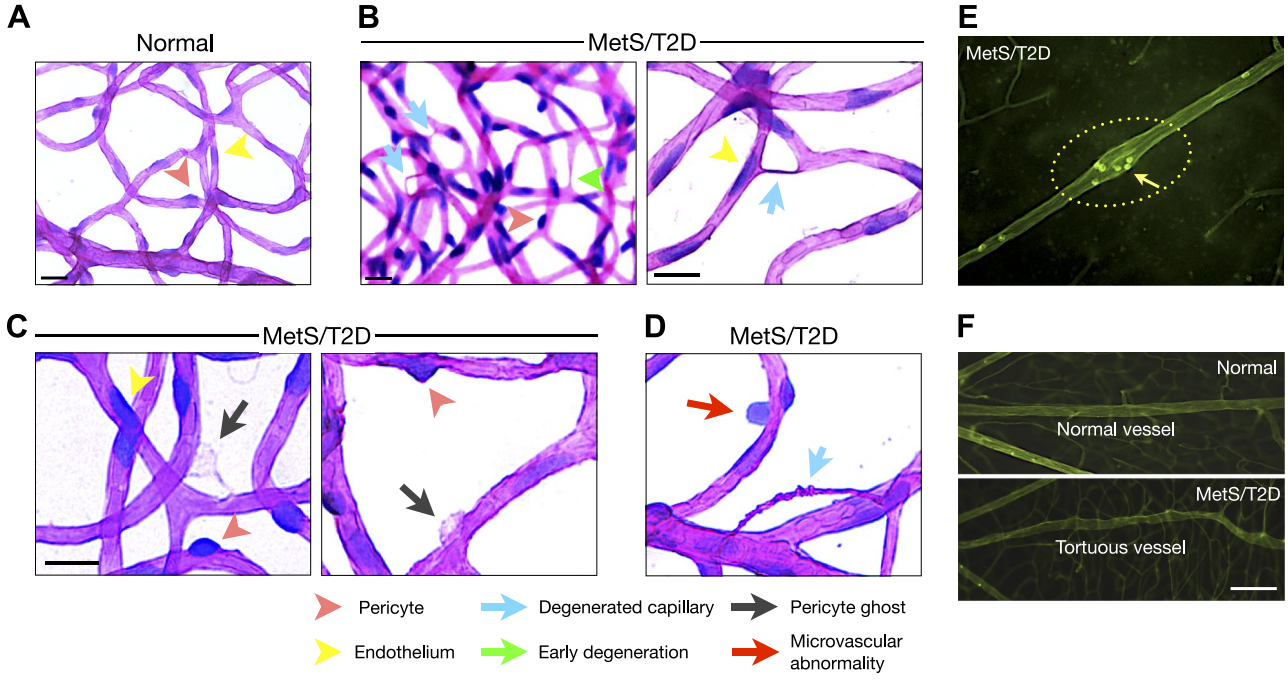


**Figure 8.** Vascular pathology in diabetic NGRs. Diabetes-induced degenerative vascular changes were visualized in flat mounts of trypsin-digested retinas. *A*) PAS- and hematoxylin-stained flat mounts of trypsin-digested retinas. Normal, nondiabetic animals showed patent retinal capillaries, composed of endothelial cells and surrounded by pericytes. Scale bar = 50 μm. *B*) T2D/MeS animals showed acellular capillaries, a hallmark of DR. Green arrow, a capillary in an early stage of degeneration; turquoise arrow, obliterated capillaries that are no longer patent. Scale bar = 50 μm. *C*, *D*) Pericyte ghosts (*C*) and microvascular wall defects (*D*) in retinas of T2D/MeS animals. Scale bar = 50 μm. *E*) Retinal flat mounts of FITC-ConA–perfused animals, showing widened sections of retinal arterioles in diabetic animals, indicative of early structural damages. Arrow, leukocyte accumulation in the arterial abnormality. *F*) Venous irregularities in diabetic NGRs. In contrast to normal animals (top panel), diabetic NGRs showed tortuous vessels (bottom panel), which has also been reported in human DR (29). Scale bar = 100 μm.

and tortuosity were observed in the diabetic NGRs (Fig. 8*F*), which have also been reported in human DR (29).

## DISCUSSION

The growing epidemic of T2D and MetS necessitates the study of these conditions in realistic models (31). Most diabetic morbidity and mortality are due to its complications. Previously, we established NGR as a model of spontaneous diet-induced MetS/T2D that exhibits all pillars of the human disease (20, 27). The NGR is a powerful surrogate for the human disease and an asset to a wide variety of investigations. The present study shows the close resemblance of the retinal lesions in diabetic NGRs with the human condition and sheds new light on the role of inflammation in the retinopathy that follows the onset of MetS/T2D.

ICAM-1 is up-regulated in STZ-induced diabetes and has been proposed to mechanistically underlie DR pathogenesis (17). In contrast to the existing paradigm, in this model of spontaneous MetS/T2D, ICAM-1 did not correlate with the diabetic state, either in early-onset or moderate diabetes. In fact, ICAM-1 decreased in advanced disease, possibly because of endothelial dysfunction. The lack of a correlation between ICAM-1 and the diabetic state casts doubt on the proposed role of this molecule in the pathogenesis, for instance in capillary plugging (32). However, independent of ICAM-1, the diabetic state can facilitate capillary plugging, for instance by directly affecting leukocytes because of structural changes or activation (33). In comparison, VCAM-1 remained unchanged in the NGRs with diabetes. VCAM-1 is expressed by endothelial cells and pericytes (34), and its level increases in ocular inflammation (35). The question arises, without ICAM-1 or VCAM-1 up-regulation, which molecules or endothelial surface moieties are responsible for the substantial arterial leukocyte adhesion in retinal vessels of the diabetic NGRs.

A key finding was that, in the diabetic NGRs, leukocytes accumulated predominantly in retinal arteries as opposed to the veins. The arterial injury in MetS/T2D NGRs may be due in part to the dyslipidemia and hypertension in these animals (20). In STZ-induced T1D, leukocytes are primarily found in the retinal veins (23). The leukocytes in the veins do not explain capillary plugging, since they are beyond the capillary circulation. In contrast, the substantial leukocyte accumulation in arteries of the diabetic NGRs could explain the arterial damage seen in humans (25), as well as the proposed capillary plugging in DR.

Notably, leukocyte accumulation negatively correlated with the disease state. In contrast to the T1D model, where leukostasis progresses with the disease duration (36), in the MetS/T2D NGRs, leukostasis significantly diminished with advanced disease. Furthermore, this reduction occurred in the retinal arteries, whereas the leukostasis in the retinal veins remained unchanged. The reduction in the arteries may be due to anti-inflammatory mechanisms in the organism that could take place to resolve the existing inflammation (37). This finding could become consequential for future therapeutic approaches and suggests that leukostasis has only a temporally limited function in early DR. Similarly, at high plasma TGs and cholesterol levels, leukocyte accumulation in retinal arteries was significantly lower. A clue to understanding these findings is that high retinal leukocyte accumulation was found only with high insulin levels. This finding suggests that, in the course of becoming insulin resistant, the hyperinsulinemia could contribute to the arterial inflammation. In the subsequent low insulin stage, the accumulation of leukocytes in arteries returns to normal.

In insulin resistance, enough insulin is secreted to maintain glucose homeostasis (1). Our results point toward an unknown side effect of this insulin outpouring, the reactive leukocyte accumulation in retinal vessels. Counterintuitively, the drop in plasma insulin in T2D diabetes may help reduce retinal inflammation. If so, the prediabetic insulin resistance during MetS could set the stage for the ensuing retinopathy. This finding is of potential clinical relevance, as it will help to prevent the retinopathy at the most effective time.

Retinal leukocyte accumulation correlated positively with plasma leptin, an indicator of body fat (38), and was significantly increased at higher leptin levels. This result could in part explain the reduction in leukocyte accumulation in late-stage disease, as animals drastically lose body fat and consequently exhibit lower leptin values in the late stages of the disease (39).

Last, the diabetic NGRs showed endothelial injury primarily in the retinal capillaries. The capillaries are critical morphologic sites, from which proliferative neovascular changes occur (40). Vessels of diabetic NGRs showed tortuosity, a known marker of human disease (29). Furthermore, the diabetic NGR retinas showed widened arterial regions, acellular capillaries, pericyte ghosts, and various microvascular abnormalities.

This work shows the suitability of the NGR for mechanistic investigations of retinal complications of MetS/T2D. Our data provide new insights about adhesion molecule expression and leukocyte accumulation in the retinas of diabetic animals. FJ

The authors thank A. Schering, F. Xie, A. Auerbach, J. Bolsinger, and A. Pronczuk for technical assistance, and R. Garland for help with manuscript preparation. This work was supported by the U.S. National Institutes of Health (NIH) DiaComp award (to A.H.-M.), overseas research fellowship awards from Bausch & Lomb (Rochester, NY, USA; to K.N. and S.N.), a fellowship award from the Japanese Eye Bank Association (to K.N. and S.N.), a Tear Film and Ocular Surface Society Young Investigator fellowship (to S. N. under the mentorship of A.H.-M.), and by the Malaysian Palm Oil Board and the Bright Focus Foundation.

## REFERENCES

1. Biddinger, S. B., and Kahn, C. R. (2006) From mice to men: insights into the insulin resistance syndromes. *Annu. Rev. Physiol.* **68,** 123–158
2. Gesta, S., Tseng, Y. H., and Kahn, C. R. (2007) Developmental origin of fat: tracking obesity to its source. *Cell* **131,** 242

3. Reaven, G. (2004) The metabolic syndrome or the insulin resistance syndrome?—different names, different concepts, and different goals. *Endocrinol. Metab. Clin. North. Am.* **33,** 283–303
4. Mizutani, M., Kern, T. S., and Lorenzi, M. (1996) Accelerated death of retinal microvascular cells in human and experimental diabetic retinopathy. *J. Clin. Invest.* **97,** 2883–2890
5. Antonetti, D. A., Barber, A. J., Bronson, S. K., Freeman, W. M., Gardner, T. W., Jefferson, L. S., Kester, M., Kimball, S. R., Krady, J. K., LaNoue, K. F., Norbury, C. C., Quinn, P. G., Sandirasegarane, L., and Simpson, I. A. (2006) Diabetic retinopathy: seeing beyond glucose-induced microvascular disease. *Diabetes* **55,** 2401–2411
6. Coleman, D. L., and Hummel, K. P. (1973) The influence of genetic background on the expression of the obese (Ob) gene in the mouse. *Diabetologia* **9,** 287–293
7. Dulin, W. E., and Wyse, B. M. (1970) Diabetes in the KK mouse. *Diabetologia* **6,** 317–323
8. Coleman, D. L., and Hummel, K. P. (1974) Hyperinsulinemia in pre-weaning diabetes (db) mice. *Diabetologia* **10**(Suppl), 607–610
9. Portha, B., Serradas, P., Bailbe, D., Suzuki, K., Goto, Y., and Giroix, M. H. (1991) Beta-cell insensitivity to glucose in the GK rat, a spontaneous nonobese model for type II diabetes. *Diabetes* **40,** 486–491
10. Ikeda, H., Shino, A., Matsuo, T., Iwatsuka, H., and Suzuoki, Z. (1981) A new genetically obese-hyperglycemic rat (Wistar fatty). *Diabetes* **30,** 1045–1050
11. Kawano, K., Hirashima, T., Mori, S., Saitoh, Y., Kurosumi, M., and Natori, T. (1992) Spontaneous long-term hyperglycemic rat with diabetic complications: Otsuka Long-Evans Tokushima Fatty (OLETF) strain. *Diabetes* **41,** 1422–1428
12. Sasase, T., Ohta, T., Ogawa, N., Miyajima, K., Ito, M., Yamamoto, H., Morinaga, H., and Matsushita, M. (2006) Preventive effects of glycaemic control on ocular complications of spontaneously diabetic Torii rat. *Diabetes Obes. Metab.* **8,** 501–507
13. Robertson, R. P., Gavareski, D. J., Henderson, J. D., Porte, D., Jr., and Bierman, E. L. (1973) Accelerated triglyceride secretion: a metabolic consequence of obesity. *J. Clin. Invest.* **52,** 1620–1626
14. Schroder, S., Palinski, W., and Schmid-Schonbein, G. W. (1991) Activated monocytes and granulocytes, capillary nonperfusion, and neovascularization in diabetic retinopathy. *Am. J. Pathol.* **139,** 81–100
15. Miyamoto, K., Hiroshiba, N., Tsujikawa, A., and Ogura, Y. (1998) In vivo demonstration of increased leukocyte entrapment in retinal microcirculation of diabetic rats. *Invest. Ophthalmol. Vis. Sci.* **39,** 2190–2194
16. Barouch, F. C., Miyamoto, K., Allport, J. R., Fujita, K., Bursell, S. E., Aiello, L. P., Luscinskas, F. W., and Adamis, A. P. (2000) Integrin-mediated neutrophil adhesion and retinal leukostasis in diabetes. *Invest. Ophthalmol. Vis. Sci.* **41,** 1153–1158
17. Miyamoto, K., Khosrof, S., Bursell, S. E., Rohan, R., Murata, T., Clermont, A. C., Aiello, L. P., Ogura, Y., and Adamis, A. P. (1999) Prevention of leukostasis and vascular leakage in streptozotocin-induced diabetic retinopathy *via* intercellular adhesion molecule-1 inhibition. *Proc. Natl. Acad. Sci. U. S. A.* **96,** 10836–10841
18. McLeod, D. S., Lefer, D. J., Merges, C., and Lutty, G. A. (1995) Enhanced expression of intracellular adhesion molecule-1 and P-selectin in the diabetic human retina and choroid. *Am. J. Pathol.* **147,** 642–653
19. Hughes, J. M., Brink, A., Witmer, A. N., Hanraads-de Riemer, M., Klaassen, I., and Schlingemann, R. O. (2004) Vascular leucocyte adhesion molecules unaltered in the human retina in diabetes. *Br. J. Ophthalmol.* **88,** 566–572
20. Noda, K., Melhorn, M. I., Zandi, S., Frimmel, S., Tayyari, F., Hisatomi, T., Almulki, L., Pronczuk, A., Hayes, K. C., and Hafezi-Moghadam, A. (2010) An animal model of spontaneous metabolic syndrome: Nile grass rat. *FASEB J.* **24,** 2443–2453
21. Chen, W., Jump, D. B., Grant, M. B., Esselman, W. J., and Busik, J. V. (2003) Dyslipidemia, but not hyperglycemia, induces inflammatory adhesion molecules in human retinal vascular endothelial cells. *Invest. Ophthalmol. Vis. Sci.* **44,** 5016–5022
22. Taylor, P. D., Wickenden, A. D., Mirrlees, D. J., and Poston, L. (1994) Endothelial function in the isolated perfused mesentery and aortae of rats with streptozotocin-induced diabetes: effect of treatment with the aldose reductase inhibitor, ponalrestat. *Br. J. Pharmacol.* **111,** 42–48
23. Miyahara, S., Kiryu, J., Yamashiro, K., Miyamoto, K., Hirose, F., Tamura, H., Katsuta, H., Nishijima, K., Tsujikawa, A., and Honda, Y. (2004) Simvastatin inhibits leukocyte accumulation and vascular permeability in the retinas of rats with streptozotocin-induced diabetes. *Am. J. Pathol.* **164,** 1697–1706
24. Jariyapongskul, A., Patumraj, S., and Niimi, H. (2003) Cerebral endothelial dysfunction in diabetes: intravital microscopic analysis using streptozotocin-induced diabetic rats. *Clin. Hemorheol. Microcirc.* **29,** 331–335
25. Nguyen, T. T., and Wong, T. Y. (2009) Retinal vascular changes and diabetic retinopathy. *Curr. Diab. Rep.* **9,** 277–283
26. Chaabo, F., Pronczuk, A., Maslova, E., and Hayes, K. (2010) Nutritional correlates and dynamics of diabetes in the Nile rat (*Arvicanthis niloticus*): a novel model for diet-induced type 2 diabetes and the metabolic syndrome. *Nutr. Metab. (Lond.)* **7,** 29
27. Bolsinger, J., Pronczuk, A., and Hayes, K. C. (2013) Dietary carbohydrate dictates development of type 2 diabetes in the Nile rat. *J. Nutr. Biochem.* **24,** 1945–1952
28. Skondra, D., Noda, K., Almulki, L., Tayyari, F., Frimmel, S., Nakazawa, T., Kim, I. K., Zandi, S., Thomas, K. L., Miller, J. W., Gragoudas, E. S., and Hafezi-Moghadam, A. (2008) Characterization of azurocidin as a permeability factor in the retina: involvement in VEGF-induced and early diabetic blood–retinal barrier breakdown. *Invest. Ophthalmol. Vis. Sci.* **49,** 726–731
29. Sasongko, M. B., Wong, T. Y., Nguyen, T. T., Cheung, C. Y., Shaw, J. E., and Wang, J. J. (2011) Retinal vascular tortuosity in persons with diabetes and diabetic retinopathy. *Diabetologia* **54,** 2409–2416
30. Hammes, H. P., Lin, J., Renner, O., Shani, M., Lundqvist, A., Betsholtz, C., Brownlee, M., and Deutsch, U. (2002) Pericytes and the pathogenesis of diabetic retinopathy. *Diabetes* **51,** 3107–3112
31. Amos, A. F., McCarty, D. J., and Zimmet, P. (1997) The rising global burden of diabetes and its complications: estimates and projections to the year 2010. *Diabet. Med.* **14**(Suppl. 5), S1–S85
32. Adamis, A. P. (2002) Is diabetic retinopathy an inflammatory disease? *Br. J. Ophthalmol.* **86,** 363–365
33. Masuda, M., Murakami, T., Egawa, H., and Murata, K. (1990) Decreased fluidity of polymorphonuclear leukocyte membrane in streptozocin-induced diabetic rats. *Diabetes* **39,** 466–470
34. Garmy-Susini, B., Jin, H., Zhu, Y., Sung, R. J., Hwang, R., and Varner, J. (2005) Integrin alpha4beta1-VCAM-1-mediated adhesion between endothelial and mural cells is required for blood vessel maturation. *J. Clin. Invest.* **115,** 1542–1551
35. Hafezi-Moghadam, A., Noda, K., Almulki, L., Iliaki, E. F., Poulaki, V., Thomas, K. L., Nakazawa, T., Hisatomi, T., Miller, J. W., and Gragoudas, E. S. (2007) VLA-4 blockade suppresses endotoxin-induced uveitis: in vivo evidence for functional integrin up-regulation. *FASEB J.* **21,** 464–474
36. Ishida, S., Usui, T., Yamashiro, K., Kaji, Y., Ahmed, E., Carrasquillo, K. G., Amano, S., Hida, T., Oguchi, Y., and Adamis, A. P. (2003) VEGF164 is proinflammatory in the diabetic retina. *Invest. Ophthalmol. Vis. Sci.* **44,** 2155–2162
37. Serhan, C. N., Chiang, N., and Van Dyke, T. E. (2008) Resolving inflammation: dual anti-inflammatory and pro-resolution lipid mediators. *Nat. Rev. Immunol.* **8,** 349–361
38. Chen, H., Charlat, O., Tartaglia, L. A., Woolf, E. A., Weng, X., Ellis, S. J., Lakey, N. D., Culpepper, J., Moore, K. J., Breitbart, R. E., Duyk, G. M., Tepper, R. I., and Morgenstern, J. P. (1996) Evidence that the diabetes gene encodes the leptin receptor: identification of a mutation in the leptin receptor gene in db/db mice. *Cell* **84,** 491–495
39. Faggioni, R., Feingold, K. R., and Grunfeld, C. (2001) Leptin regulation of the immune response and the immunodeficiency of malnutrition. *FASEB J.* **15,** 2565–2571
40. Hammes, H. P., Feng, Y., Pfister, F., and Brownlee, M. (2011) Diabetic retinopathy: targeting vasoregression. *Diabetes* **60,** 9–16

*Received for publication August 1, 2013.*
*Accepted for publication February 3, 2014.*